Coastal Engineering 60 (2012) 227–234

Contents lists available at SciVerse ScienceDirect

Coastal Engineering

journal homepage: www.elsevier.com/locate/coastaleng

Improving storm surge estimates: Increased downwards transfer of horizontal momentum by wind-driven waves

David P. Callaghan *, Peter Nielsen, Tom E. Baldock

School of Civil Engineering, The University of Queensland, Brisbane, 4072, Australia

ARTICLE INFO

Article history:
Received 18 July 2011
Received in revised form 5 October 2011
Accepted 19 October 2011
Available online 22 November 2011

Keywords:
Wind waves
Reynolds stress
Wind stress
Storm surge
Numerical modelling

ABSTRACT

The numerical predictions of historical storm surges in which the low pressure meteorological system remains well offshore requires a factor three, or more, wind stress than that provided using the standard wind stress coefficients found in the literature. The literature values are from the 'air side', where wind stress coefficients are determined either from the measured vertical velocity gradient of the wind over the water or more commonly from wind Reynolds stresses. On the other hand, the wind stress required to match the observed storm surges is consistent with the momentum transfer observed during wind-wave growth experiments (i.e., the inferred wind stress coefficients from experiments measuring wave height growth due to wind). Both the wind-wave growth data and our storm surge modelling are consistent with field and laboratory measurements of Reynolds stresses of wind-driven waves. The possibility that there is more momentum being transferred downwards urges the development of a storm surge model capable of using the wind stress inferred from the wind-wave growth data. This requires a Reynolds stress model covering deep through to shallow water depths and at arbitrary levels (3D model implementation), which has been formulated herein. Application of this wind stress to Tropical Cyclone Roger using the steady shallow water equations qualitatively explains the observed storm surge. This new approach also raises the question of why storm surge estimates are generally acceptable for weather systems that cross the coastline despite the use of momentum transfer based on air side wind stress.

1. Introduction

In order to generate ocean currents and storm surges, a mechanism for transferring horizontal momentum downwards in the water column is required. This is quantified by $\overline{uw}$, where the velocity notation uses $u(t) = \bar{u} + \tilde{u} + u'$ to distinguish, steady, periodic and random velocity components. Turbulent diffusion is one mechanism available for this transfer with

$$\tau_{turbulent} = \rho \nu_t \frac{\partial \bar{u}}{\partial z} = -\rho \overline{u' w'} \tag{1}$$

where $\tau_{turbulent}$ is the shear stress, ρ is the water density, ν_t is the eddy viscosity and $\frac{\partial \bar{u}}{\partial z}$ is the mean velocity gradient (Fig. 1). The other potential mechanism is through the oscillatory motion Reynolds stress

$$\tau_{wave} = -\rho \overline{\tilde{u}\tilde{w}}. \tag{2}$$

While wave propagation with constant form involves horizontal ($\tilde{u}$) and vertical ($\tilde{w}$) velocities that are in quadrature and hence there are no Reynolds stresses $\left(\tau_{wave} = -\rho\overline{\tilde{u}\tilde{w}} = 0\right)$ available for downwards transfer of horizontal momentum (see, for example, Nielsen, 2009), standing and partially standing waves do have Reynolds stresses that drive steady circulation cells half a wave length long (Carter et al., 1973). Nielsen et al. (2011) used an uneven pressure distribution on the water surface argued for by Miles (1957) and others to show that in the shallow water limit and when wave height grows in the downwind direction, that $\overline{\tilde{u}\tilde{w}} < 0$ and hence $\tau_{wave} > 0$. They also showed that when the wave height grows exponentially in time but is uniform in space, $\tau_{wave} = -\rho\overline{\tilde{u}\tilde{w}} = 0$. The Reynolds stress estimates due to spatial wave growth had a similar order of magnitude as field (Cavaleri and Zecchetto, 1987) and laboratory (Shonting, 1970) measurements. In addition, the theory is in qualitative agreement with Cavaleri and Zecchetto's observed phased lead of η ahead of $\tilde{u}$.

There are two rich data sources for estimating momentum transfer between the atmosphere and the ocean. They are the 'wave height growth' measurements (measuring wave height changes in the absence of wave breaking in space) and the 'air side' wind shear measurements (measuring wind stress above the air/water boundary interface and assuming that this air side stress applies at the water surface). Wave height growth data indicates two to three times

* Corresponding author. Tel.: +61 7 33653517; fax: +61 7 33654599.
E-mail address: dave.callaghan@uq.edu.au (D.P. Callaghan).

0378-3839/$ – see front matter © 2011 Elsevier B.V. All rights reserved.
doi:10.1016/j.coastaleng.2011.10.004

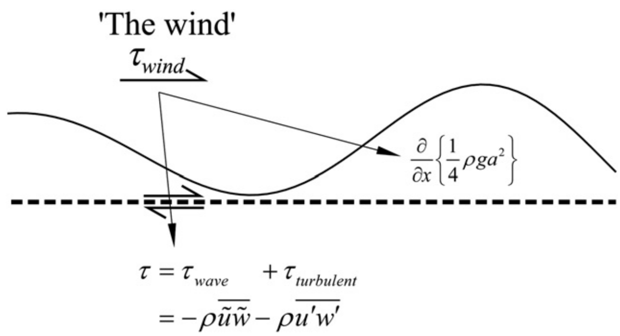

Fig. 1. The wind shear τ_{wind} is transferred to the ocean with part of the input above the wave trough level (dashed line) and the remaining momentum being transferred to below the wave trough level through τ_{wave} and $\tau_{turbulent}$.

more momentum input from the wind to the water column compared to the air side τ_{wind} (Belcher and Hunt, 1998), with the additional wave height growth measurements since (Peirson and Garcia, 2008) maintaining this discrepancy. The air side τ_{wind} also indicates lower momentum transfer than Cavaleri and Zecchetto (1987) Reynolds stress measurements (Nielsen et al., 2011).

A consequence of forcing storm surge models with air side estimated τ_{wind} should be an underestimated storm surge. However, the literature is full of examples where the air side τ_{wind} combined with parametric wind fields of meteorological systems that cross the coastline apparently suffice in hindcasting observed storm surges (e.g., Sheng et al., 2010). Nevertheless, modelling of two storm surge events off the eastern Australian coast (Tropical Cyclone Roger and the February 1996 East Coast Low) in which the “eye” or low pressure did not cross the coast but remained hundreds of kilometres offshore is inadequately hindcasted when the numerical model is forced by air side τ_{wind} derived from hindcast winds. The storm surge (defined as the water surface level less the astronomical tide) estimates for these two events are less than half to that measured (Stewart, 2010; Stewart et al., 2010) when using air side τ_{wind}. While many other short-comings of Stewart et al.'s models (Stewart, 2010; Stewart et al., 2010) may explain this, those have been investigated at length (Stewart et al., 2010) and found to involve only nominal changes in the estimated storm surge. Thus, Stewart's numerical modelling also supports the need for greater input of momentum from the wind compared to the air side τ_{wind}. Our argument then, given the Cavaleri and Zecchetto (1987) data and the wave height growth measurements agrees on the magnitude of the Reynolds stresses, these are investigated for predicting storm surges. For two-dimensional models, an expression for τ_{wind} at the mean water surface will be developed. For three-dimensional models, a distribution of τ_{wind} through the ocean depth will be developed.

1.1. Momentum transfer from the atmosphere to the ocean

Wave radiation stress is the excess pressure force compared to the still water situation plus the horizontal momentum flux (Longuet-Higgins and Stewart, 1960, 1964; Lundgren, 1963). Wave radiation stress, or its ability to push, is more often seen by what it does, e.g., the driver of longshore currents when waves break at an angle to the beach and increases in the mean water surface level that occurs through the surf zone. Waves that are growing in the downwind direction (due to the action of wind) have a downward transfer of x-momentum by Reynolds stresses τ_{wave} from the oscillatory wave motion, which can be quantified for the situation where there is no mean current ($\bar{u} = 0$), the mean water surface is horizontal ($\partial\bar{\eta}/\partial x = 0$), no wave breaking and $\tau_{turbulent} \approx 0$. The momentum transferred from the wind is then in force balanced with the wave radiation stress gradient, i.e.,

$$\tau_{wind} = \frac{\partial S_{xx}}{\partial x} \tag{3}$$

(see Fig. 2A). Longuet-Higgins and Stewart (1964), when deriving their wave radiation stress, included three contributions of

$$S_{xx} = S_{xx}^{(1)} + S_{xx}^{(2)} + S_{xx}^{(3)} \tag{4}$$

where

$$S_{xx}^{(3)} = \frac{1}{4}\rho g a^2 \tag{5}$$

comes from pressure fluctuations above the mean water level and

$$S_{xx}^{(1)+(2)} = \rho g \frac{a^2}{4} \times \frac{4kh}{\sinh 2kh} \tag{6}$$

is from pressure and velocity fluctuations below the mean water surface level. Here, the notation is following that of Longuet-Higgins and Stewart (1964), a is the wave amplitude, g is the gravitational acceleration, h is the mean water depth, and k is the wave number, all real-valued. Part of the wind stress will be balanced by $\partial(\rho g a^2/4)/\partial x$ above the mean water surface level (Figs. 1 and 2A) with the remaining momentum from the wind stress being transferred further downwards (Fig. 2A). Consequently, at the mean water surface level and ignoring turbulent diffusion, the Reynolds stress equals $\partial S_{xx}^{(1)+(2)}/\partial x$ or

$$-\rho\overline{\tilde{u}\tilde{w}}\Big|_{z=0} = \alpha\rho g \frac{a^2}{4} \times \frac{4kh}{\sinh 2kh} \tag{7}$$

where α is the exponential growth rate observed in wave growth experiments (Peirson and Garcia, 2008). The Reynolds stress at the mean water surface level, as a fraction of the wave radiation stress, thus varies from 2/3 in the shallow water limit to vanishing in the deep water limit (Fig. 2B) according to sine wave theory. The wave growth experiments measure the wave amplitude growth rate α for this situation and then this is converted into Miles' (1957) normalised wave growth parameter β (Peirson and Garcia, 2008). That is, while the waves in Miles' (1957) model grow in time,

$$\eta = A_0 e^{\beta t} \cos(\omega t - kx) \tag{8}$$

the parameters are obtained from spatial growth rates of

$$\eta = A_0 e^{\alpha x} \cos(\omega t - kx) \tag{9}$$

where A_0 is the initial wave amplitude and ω is the angular frequency.

Waves propagating across the ocean eventually reach quasi-equilibrium (albeit with growing period) while still being forced by the wind. One simplistic way of conceptualising this quasi-equilibrium state is: from time to time waves break (white-capping) and then grow until breaking again, with the post-breaking wave height being similar to the wave height when growth commenced on the previous cycle (Fig. 3). This conceptual model balances wave growth and wave dissipation, where additional wave energy is dissipated but the momentum transferred from the atmosphere to the waves is subsequently transferred to the water column. As a first approximation, we assume that the momentum input is the same as in the growing non-breaking waves discussed above. The cycle results in radiation stress being approximately constant when spatially averaged over a growing-breaking cycle (Fig. 3). Consequently, radiation stresses are no longer available to balance τ_{wind}. The momentum accumulated during the growth phase becomes a combination of $\bar{u}$

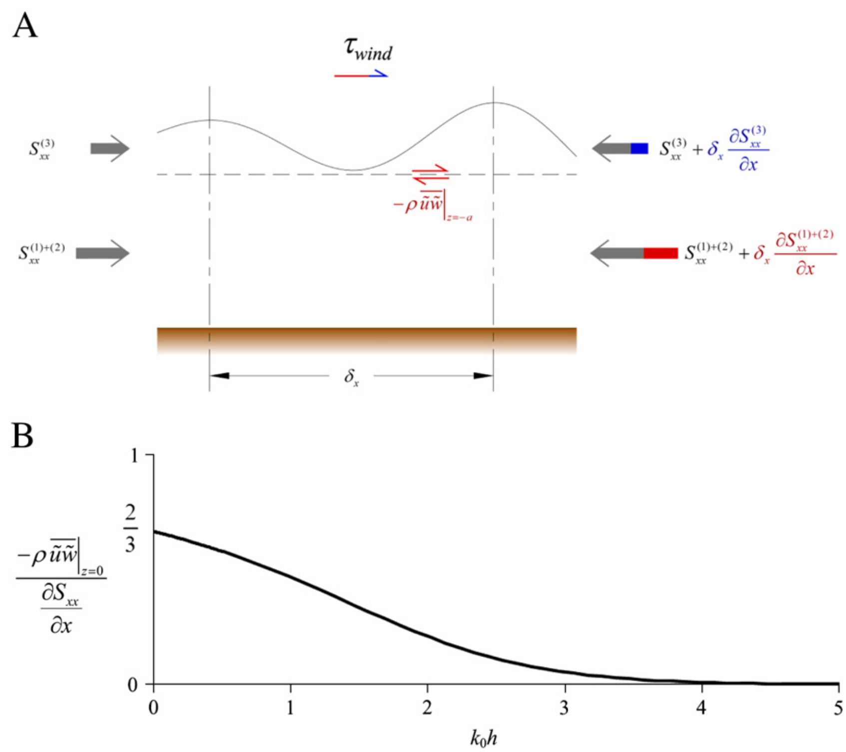

Fig. 2. A) Force balance between wind stress and radiation stress gradient for non-breaking growing waves with zero mean current and mean water level gradient $\left(\bar{u} = 0, \frac{\partial \bar{\eta}}{\partial x} = 0\right)$. The radiation stress contributions are differentiated by colour with blue above and red below the mean water surface level. B) The ratio of Reynolds stress at the mean water surface level and wave radiation stress gradient.

acceleration (possibly variable with depth), mean water surface gradients $\partial\bar{\eta}/\partial x$ and bed shear stress resulting from the subsequent currents, again in a spatially averaged sense.

In deep water, the infused momentum remains, according to sine wave theory, above the wave trough level (i.e., $\rho\overline{\tilde{u}\tilde{w}}|_{z=-a} = 0$). During the breaking phase, downwards momentum transfer is limited to turbulent diffusion of $-\rho\overline{u'w'}|_{z=-a}$. One possible approach to estimate the storm surge is to spatially average the momentum transfer (over several growing-breaking cycles) and apply it to the mean water surface control volume, forced by a combination of Reynolds stress and the momentum infused above the wave trough level. The linear wave theory presented above implies that in deep water, the momentum transfer is predominantly by turbulent diffusion and as the water depth decreases, the Reynolds stress will take over as the primary transfer mechanism. This approach requires a Reynolds stress model valid for deep through to shallow water depths.

Melville (1996), when discussing the transfer of momentum from the wind to the wave and to turbulent diffusion, highlighted Mitsuyasu's (1985) conjecture that up to 90% of the momentum from the wind is lost from the wave field (into turbulent diffusion) by wave breaking in the generation region. While there are many more details requiring refinement (i.e., increase of wave period with fetch, non-sinusoid waves), it would appear that the proposed model has, as a proof of concept, some support from previous findings. Nevertheless, further analytical work and field measurements are required to extend and verify the Reynolds stress model and storm surge prediction method presented herein before commercial application.

The paper is arranged as follows. The Reynolds stress model is formulated in Section 2 by extending the work of Nielsen et al. (2011). In this section, we compare air side wind stress coefficients to Reynolds stress coefficients for weather conditions typical of Tropical Cyclone (TC) Roger. Section 3 implements a new wind stress forced storm surge models and estimates the cross-shore storm surge height profiles for both air side and wave height growth τ_{wind}. The implications of applying the wind stress for storm surge estimates near Surfers Paradise, located in Queensland, Australia, are discussed in Section 4, where we reconcile historical events with previous statistical modelling. A brief summary and ideas for future research are communicated in Section 5.

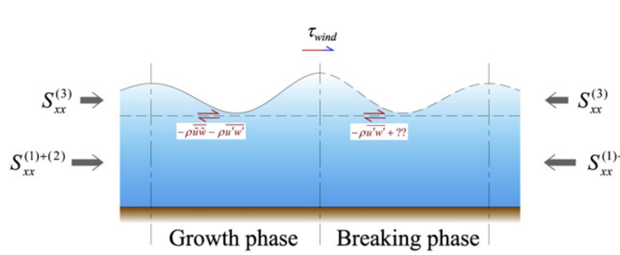

Fig. 3. Quasi-steady wave breaking (white-capping) followed by growth until further wave breaking. The wave radiation stress not available for balancing horizontal momentum is transferred to the water column during the growth phase (blue and red additions to S_{xx} shown illustrated in Fig. 2).

2. Momentum transfer formulation

The Reynolds stress model formulation is divided into shallow water (Section 2.1) and arbitrary depth (Section 2.2) expressions. Both sections will extend the previous work by Nielsen et al. (2011) and additionally, Section 2.2 includes comparisons with Sanchez-Arcilla et al. (1992) Reynolds stress formulation and a numerical check of our new Reynolds stress model. Section 2.3 complements the Reynolds stress model by formulating the total transferred momentum from the atmosphere to the ocean by adding terms relevant above wave trough level to the Reynolds stress at the wave trough level.

2.1. Momentum transfer below the wave trough level in the shallow water limit

Nielsen et al. (2011) estimated the Reynolds stress below the mean water surface level of a "sine wave" growing in the downwind direction as

$$-\rho\overline{\tilde{u}\tilde{w}} = \frac{\rho\alpha c^2 A_0^2 e^{2\alpha x}(z+h)}{2h^2} \tag{10}$$

where k, c and α are the wave number, phase speed and spatial growth rate, which are all real-valued, ρ is the water density, h is the mean water depth, A_0 is the initial wave amplitude, x, z and t are the space and time coordinates, with z being positive upwards and measured from the mean water level. Rewriting Eq. (10) using $A_0^2 e^{2\alpha x} = (A_0 e^{\alpha x})^2 = a^2$ where a is the local wave amplitude, the Reynolds stress near the wave trough level becomes

$$-\rho\overline{\tilde{u}\tilde{w}} = \frac{\rho\alpha c^2 a^2}{2h}. \tag{11}$$

From equating the air pressure from Miles (1957) with that used by Nielsen et al. (2011), they showed that the relationship between the spatial growth parameter α and Miles' normalised wave growth parameter β is

$$\alpha = \frac{\beta}{2}\frac{\rho_a}{\rho}\frac{U_r^2 k^2}{g} \tag{12}$$

where ρ_a is the air density and $U_r = (U_{10} - c)$ is the relative velocity, U_{10} is the wind speed at 10 m above mean water surface level and g is the gravitational acceleration. Combining Eqs. (11) and (12) and writing in the form $-\rho\overline{\tilde{u}\tilde{w}} = C_{RS} \times \rho_a U_{10}^2$ gives

$$C_{RS} = \frac{1}{4}\beta\frac{(\omega a)^2}{gh}\left(1 - \frac{c}{U_{10}}\right)^2. \tag{13}$$

2.2. Momentum transfer below the wave trough level in arbitrary depth

The expressions so far are valid in the shallow limit. To extended our Reynolds stress model to arbitrary depth, we use the Nielsen et al. (2011) proposed velocity potential (ϕ) for spatially growing waves in arbitrary depths of

$$\phi(x,z,t) = \mathrm{Re}\left\{ i\frac{g}{kc}\left(1 + \frac{P_0}{\rho g A_0}e^{ik\delta}\right) A_0 e^{(\alpha + ik)x}\frac{\cosh[(k - i\alpha)(z+h)]}{\cosh[(k-i\alpha)h]} e^{-ikct}\right\} \tag{14}$$

with corresponding water particle velocities given by $\tilde{u} = -\frac{\partial\phi}{\partial x}$ and $\tilde{w} = -\frac{\partial\phi}{\partial z}$ in the horizontal and vertical directions respectively and Eq. (14) is the usual airy wave potential for P_0, $\alpha = 0$. Here, P_0 and δ are the amplitude of the air pressure fluctuations on the wave and the phase difference between air pressure and water surface fluctuations respectively (Fig. 4).

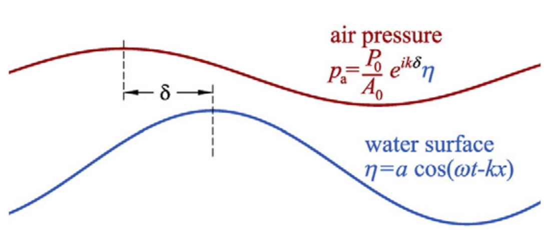

Fig. 4. Sine wave growing due to sinusoid air pressure which peaks up-wind of the crest.

The Reynolds stress that corresponds to this velocity potential is then

$$-\rho\overline{\tilde{u}\tilde{w}} = \frac{1}{2}\frac{\rho g^2 A_0^2 e^{2\alpha x}}{c^2k^2}\left(1 + \left(\frac{P_0}{\rho g A_0}\right)^2 + 2\frac{P_0}{\rho g A_0}\cos(k\delta)\right)\left(k^2 + \alpha^2\right) \times \frac{\sin[2\alpha(z+h)]}{\cosh 2kh + \cos 2\alpha h} \tag{15}$$

which is zero for $\alpha = 0$. For $kh \to 0$, $\alpha << k$ and $\frac{P_0}{\rho g A_0} << 1$ it becomes

$$\begin{aligned} -\rho\overline{\tilde{u}\tilde{w}} &= \frac{1}{2}\frac{\rho g^2 A_0^2 e^{2\alpha x}}{c^2k^2}\left(k^2 + \alpha^2\right) \times \frac{2\alpha(z+h)}{1+1} \\ &= \frac{\rho c^2 A_0^2 e^{2\alpha x}}{2h^2} \times \alpha(z+h) \end{aligned} \tag{16}$$

reproducing Nielsen et al.'s (2011) Eq. (13), repeated here as Eq. (10).

Sanchez-Arcilla et al. (1992) proposed that the Reynolds stress for spatially growing waves was

$$-\rho\overline{\tilde{u}\tilde{w}} = -\rho\frac{1}{2}\left(\frac{g}{ck}\right)^2 \times Z\frac{\partial Z}{\partial z} \times a\frac{\partial a}{\partial x} \tag{17}$$

which is different to Eq. (15) and comes from the velocity potential

$$\begin{aligned} \phi &= \Re\left\{ i\frac{g}{kc}Z(z)a(x)e^{i(kx - kct)}\right\} \\ &= \frac{g}{kc}Z(z)a(x)\sin(kx - kct) \end{aligned} \tag{18}$$

which assumes $Z(z)$ is real-valued (i.e., no velocity phase changes in the vertical). However, their velocity potential does not satisfy the continuity equation for incompressible flow $\left(\frac{\partial^2\phi}{\partial x^2} + \frac{\partial^2\phi}{\partial z^2} = 0\right)$, i.e.,

$$\frac{\partial^2\phi}{\partial x^2} + \frac{\partial^2\phi}{\partial z^2} = \frac{g}{kc}\left\{ Z\frac{\partial^2 a}{\partial x^2} + 2kZ\frac{\partial a}{\partial x}\cot(kx - kxt) - k^2 aZ + a\frac{\partial^2 Z}{\partial z^2}\right\}\sin(kx - kxt) \tag{19}$$

or using $a = A_0 e^{\alpha x}$ and $Z = \frac{\cosh k(z+h)}{\cosh kh}$,

$$\frac{\partial^2\phi}{\partial x^2} + \frac{\partial^2\phi}{\partial z^2} = \frac{\alpha g a Z}{kc}\{\alpha + 2k\cot(kx - kxt)\}\sin(kx - kxt) \tag{20}$$

which is generally non-zero. If $Z(z)$ is assumed complex (i.e., allow vertical velocity phase changes), then Eq. (17) becomes

$$-\rho\overline{\tilde{u}\tilde{w}} = -\rho\left(\frac{g}{kc}\right)^2 a(x)\left\{\begin{array}{l} \dfrac{\partial a(x)}{\partial x}\overline{\dfrac{\partial \mathrm{Re}\left\{Z(z)e^{i(kx-kct)}\right\}}{\partial z}\mathrm{Re}\left\{Z(z)e^{i(kx-kct)}\right\}} \\ +a(x)\overline{\dfrac{\partial \mathrm{Re}\left\{Z(z)e^{i(kx-kct)}\right\}}{\partial z}\dfrac{\partial \mathrm{Re}\left\{Z(z)e^{i(kx-kct)}\right\}}{\partial x}} \end{array}\right\} \tag{21}$$

and for $Z(z) = \frac{\cosh[(k - i\alpha)(z+h)]}{\cosh[(k-i\alpha)h]}$ and $a = A_0\,e^{\alpha x}$, Eq. (21) yields

$$-\rho\overline{\tilde{u}\tilde{w}} = \frac{1}{2}\frac{\rho g^2 A_0^2 e^{2\alpha x}}{c^2k^2}\left(k^2 + \alpha^2\right) \times \frac{\sin[2\alpha(z+h)]}{\cosh 2kh + \cos 2\alpha h} \tag{22}$$

which is different from Eq. (15) by the factor

$$1 + \left(\frac{P_0}{\rho g A_0}\right)^2 + 2\frac{P_0}{\rho g A_0}\cos(k\delta) \tag{23}$$

which is related to the pressure forcing being a fraction of the wave height.

Nielsen et al.'s (2011) velocity potential differs from free sine waves in that the wave number is complex and there is an additional factor $1 + \frac{P_0}{\rho g A_0}e^{ik\delta}$ required to satisfy the linearized surface boundary condition due to the non-uniform air pressure.

Reynolds stresses estimated from Eq. (15) approach zero at all levels below the wave trough level in deep water, while the radiation stresses remain finite in deep water. The momentum flux in the horizontal direction (radiation stress) is, in deep water, concentrated above the wave trough level (mathematically above mean water surface level) and originates from pressures fluctuations (see Eqs. 9 and 18 through 20 of Longuet-Higgins and Stewart, 1964). Consequently, there is approximately zero horizontal flux of momentum (radiation stress) below the wave trough level in deep water and consequently no need for further downwards flux of horizontal momentum below the wave trough level (i.e., zero Reynolds stress) as discussed in the Introduction.

To apply Eq. (15), a dispersion relationship is required to estimate k and α from ω, h and the applied wind forcing. Nielsen et al. (2011) proposed

$$(k-\alpha i)\tanh[(k-\alpha i)h]=\frac{\omega^2}{g\left(1+\frac{P_0}{\rho g A_0}e^{i\delta k}\right)} \tag{24}$$

based on their long wave equation including forcing from wave coherent air pressure. Maximum downwards transfer of horizontal momentum occurs for $k\delta=\pi/2$ with

$$\frac{P_0}{\rho g A_0}\sim\beta\frac{\rho_a}{\rho}\frac{U_r^2 k}{g}\frac{1}{\sin k\delta}. \tag{25}$$

To ensure the lengthy mathematics required to derive Eq. (15) are correct, numerical estimates of time varying $\tilde{u}$ and $\tilde{w}$ have been estimated directly from Eq. (14) by numerically differentiating Eq. (14). The time averaged product of $\overline{\tilde{u}\tilde{w}}$ was then numerically estimated from these velocities. The parameters tested are $A_0\in[0.25\text{ m};\ 5\text{ m}]$ $T\in[3\text{ s};\ 16\text{ s}]$, $h\in[1\text{ m};\ 60\text{ m}]$, $U_{10}\in[10\text{ m/s};\ 60\text{ m/s}]$ and $\frac{z}{h}\in[-0.95;0]$ using 6375 sensible combinations (i.e., $U_{10}>c$ and $k>\alpha$ and $h>2A_0$ and $\sqrt{2A_0/L}<0.14$, where L is the wavelength). The wind forcing used Eq. (25) with $\beta=32$. The spatial gradients were numerically estimated using distance increments of $\delta_x=L/10^5$ and $\delta_z=h/10^5$. The temporal increment was $\delta_t=T/10^5$, where T is the wave period. All three increments were convergent. The numerical estimates of Reynolds stresses confirm Eq. (15) (Fig. 5).

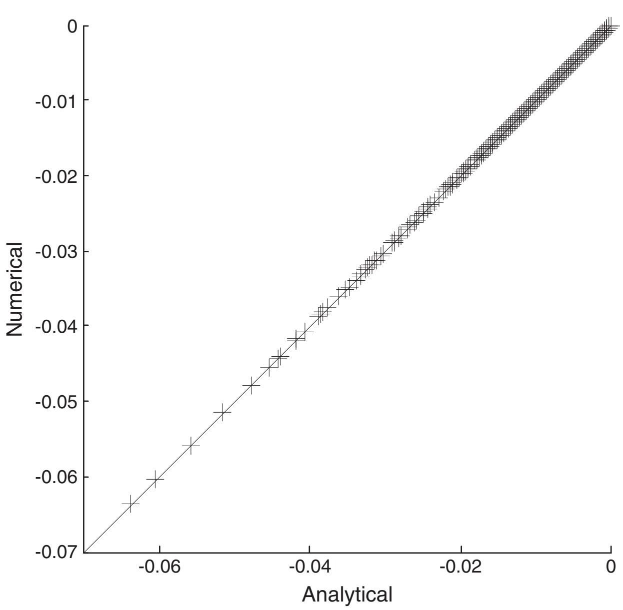

Fig. 5. Comparison of the analytically estimated $\overline{\tilde{u}\tilde{w}}$ from Eq. (15) with estimates obtained from Eq. (14) using numerical differentiating and integrating techniques. See text for parameter ranges and rules on sensibility of parameter combinations. The crosses lying on the continuous line indicates agreement between the analytical and numerical estimates of $\overline{\tilde{u}\tilde{w}}$.

2.3. Momentum transfer above the wave trough level in finite depth

For sine waves, the wind stress is partly transferred via Reynolds stress to the water column below the wave trough level (Figs. 1 and 2A) with the remainder increasing the pressure fluctuations above the wave trough level by

$$\frac{\partial S^{(3)}}{\partial x}=\frac{\partial}{\partial x}\left\{\frac{1}{4}\rho g a^2\right\} \tag{26}$$

(mathematically, $S^{(3)}$ is determined for above mean water surface level). Under $a\sim A_0 e^{\alpha x}$ growth, the momentum transferred to pressure fluctuations is

$$\tau_{wind}^{(3)}=\frac{1}{2}\alpha\rho g a^2 \tag{27}$$

where $\tau_{wind}^{(3)}$ is a proportion of the wind stress. In the quasi-equilibrium framework introduced in Section 1, the time averaged momentum is conserved, leading to the total of

$$\begin{aligned}\tau_{wind}&=\tau_{wind}^{(3)}-\rho\overline{\tilde{u}\tilde{w}}\Big|_{z=0}\\ \tau_{wind}&=\frac{1}{2}\rho g a^2\left[\alpha+\frac{g}{c^2k^2}\left(1+\left(\frac{P_0}{\rho g A_0}\right)^2+2\frac{P_0}{\rho g A_0}\cos(k\delta)\right)\left(k^2+\alpha^2\right)\right.\\ &\qquad\left.\times\frac{\sin 2\alpha h}{\cosh 2kh+\cos 2\alpha h}\right].\end{aligned} \tag{28}$$

When $\frac{P_0}{\rho g A_0}<<1$ and writing in the form $\tau_{wind}=C_{\text{wind}}\times\rho_a U_{10}^2$ gives

$$\begin{aligned}C_{\text{wind}}&=\frac{1}{2}\rho g a^2\left[\alpha+\frac{g}{c^2k^2}\left(k^2+\alpha^2\right)\times\frac{\sin 2\alpha h}{\cosh 2kh+\cos 2\alpha h}\right]\\ &\qquad\times\left(\rho_a U_{10}^2\right)^{-1}.\end{aligned} \tag{29}$$

3. An approximate implementation for storm surge estimates

In this section, we estimate storm surge elevations using τ_{wind} and C_{wind} from the wave height growth data, which exceeds the air side wind stress of $C_{10}\rho_a U_{10}^2$, and test these against TC Roger observations. Tilburg and Garvine (2004) proposed a simple method for estimating storm surges using the linear and steady shallow water equations that included surge from wind stress and along shelf currents (Coriolis). They compared their estimates to a nonlinear and unsteady numerical model for storm surges off the New Jersey coast, Atlantic City, USA. They found that the numerical model explained 79% of the measured storm surges, marginally better than the 74% explained by this analytical approach. We are unable to use their simple model directly as the continental shelf shape of the Gold Coast is different to that assumed by Tilburg and Garvine (2004). Nevertheless, applying their approach using a simplified continental shelf for the Gold Coast (Fig. 6) results in

$$\eta=\frac{fW_x}{g}\sqrt{\frac{\rho_a C_{10}W}{\rho C_{\text{B}}|W_x|}}(y+L_1)+\frac{\rho_a C_{10}W_yW}{\rho g}\left(\frac{1}{\beta_1}+\frac{1}{\beta_2}\right)\ln\frac{h_1+\beta_1 L_1}{h_1-\beta_2 y} \tag{30}$$

for $0<y<L_1$ and assuming that the storm surge at the continental shelf edge is zero. Here, η is the storm surge, see Fig. 6 for coordinate, length and slope definitions, W, W_x and W_y are wind speed and velocity in x (longshore) and y (cross-shore) directions, C_{B} is the bottom drag coefficient and f is the Coriolis parameter. As has been previously pointed out, storm surges under these assumptions are infinite (Walton Jr and Dean, 2009) for zero depth, i.e., depth is zero when $y=L_1$ and from Eq. (30) $\eta=\infty$. Consequently we take a sensible limit on depth of $h=6$ m, based on field measurements at the Gold

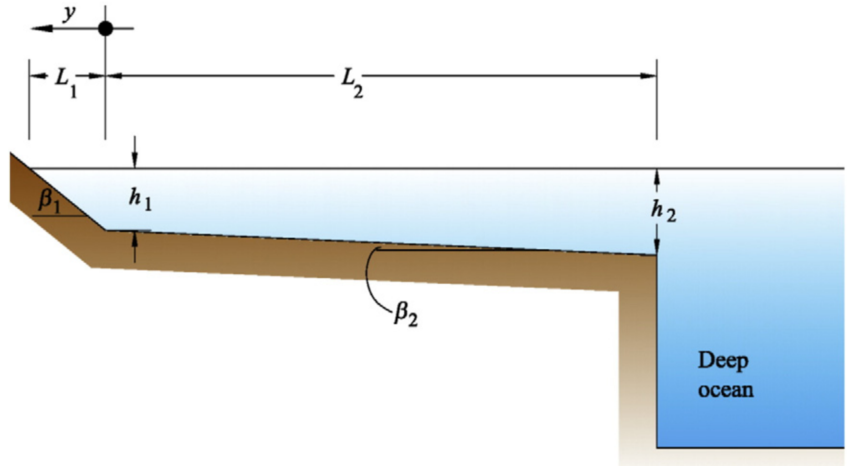

Fig. 6. Simplified continental shelf for Gold Coast, Australia, where $(L_1, L_2, h_1, h_2, \beta_1, \beta_2) = (2\text{ km}, 40\text{ km}, 26\text{ m}, 200\text{ m}, 1/77, 1/230)$.

Coast Spit (Fig. 7) that indicate that the measured water level between $h = 1.5$ m and $h = 6$ m is within a few centimetres of each other during the 2009 East Coast Low event (these measurements were obtained using the Gold Coast Spit Research Station, Cartwright et al., 2009). It is expected that at water depths less than 6 m, depth limited wave breaking was starting to occur during TC Roger and as we exclude wave radiation stress gradients from the model, the surf zone must also be excluded from the model.

To apply this model, we first calibrate Eq. (30) using the air side wind drag to Stewart et al. (2010) peak storm surge prediction of 0.24 m (also obtained using the conventional air side wind drag). This calibration removes some of the uncertainty associated with Eq. (30), as discussed by Tilburg and Garvine (2004). This process yielded an air side wind drag coefficient of $C_{10} = 2.2 \times 10^{-3}$ for $U_{10} = 19$ m/s and a wind direction of 45° to the coastline (Fig. 8), which is similar to that used by Stewart et al. (2010) (2×10^{-3}) and those recommended in the literature $(1.5 \times 10^{-3}$ to 2×10^{-3} estimated from Fig. 2 of Donelan et al. (2004)).

Modifying Eq. (30) to use C_{wind}, which varies with cross-shore location y, results in

$$\frac{\partial \eta}{\partial y} = A \times \sqrt{C_{\text{wind}}} + B \times \frac{C_{\text{wind}}}{h} \tag{31}$$

where $A = \frac{fW_x}{g}\sqrt{\frac{\rho_a W}{\rho C_B |W_x|}}$ and $B = \frac{\rho_a W_y W}{\rho g}$ are constants and C_{wind} was estimated using Eq. (29). Eq. (31) was numerically integrated using a spatially centred scheme on a variable spacing grid for TC Roger which yielded storm surges between 0.9 m at 10 m mean water depth and 1.15 m at 6 m mean water depth (Fig. 8).

The measured storm surge during TC Roger at the Gold Coast Seaway (Stewart et al., 2010) (Fig. 9, continuous line) peaked at 0.76 m, with a range of between 0.4 m and 0.76 m near the peak. The low-pass-filtered-storm-surge peak is 0.55 m (Fig. 9, – – – –). The predicted storm surge estimated from air side stress underestimates the measured storm surge (Fig. 9, – – –). In comparison, using τ_{wind} from the wave height growth data provides estimates above the low-pass-filtered peak when in water depths well outside (Fig. 9, - - - - -) the surf zone limit.

The storm surge models of Eqs. (30) and (31) both assume depth averaged currents. The momentum flux entering at the water surface, in these models, is immediately available to drive currents near the sea bed, and for shallow water depths, this approach is well established. The sine wave theory presented here, however, concentrates the wind stress transfer to pressure fluctuations above the wave trough level, which is, after being released (wave breaking), transferred further downwards by turbulent diffusion. Hence, there is less potential to drive full depth longshore currents (to generate surge from Coriolis force). For example, TC Roger wave conditions need turbulent diffusion for momentum transfer at depths greater than *ca* 50 m for depth averaged longshore currents to develop, which requires a mean water surface gradient to balance the Coriolis force. If we assume that there is no wind driven storm surge at 50 m depth, then the storm surge predictions at 10 m and 6 m water mean water depth are 0.49 m and 0.75 m respectively. To test 3D relaxation of longshore surge component (Coriolis), Eqs. (27) and (22) would

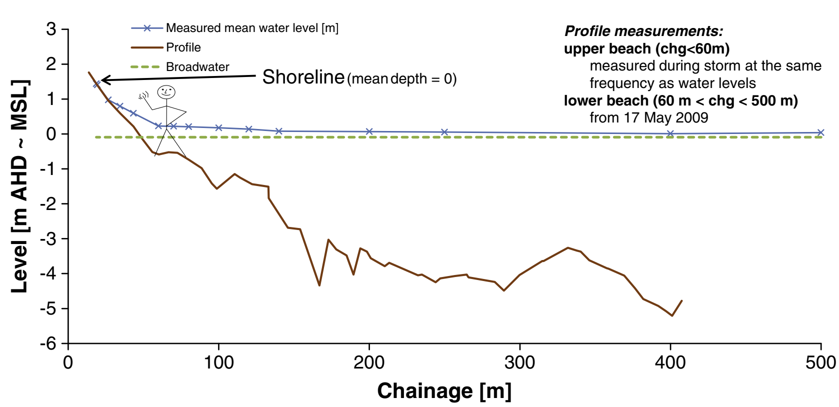

Fig. 7. Measured cross-shore exposed coast (—×—) mean water level profile during the 2009 East Coast Low event of the Gold Coast at the Spit on 21 May 2009 at 12 pm with the measured water levels in the Broadwater (– – –). The beach profile (——) and a 2 m tall person is shown for scale.

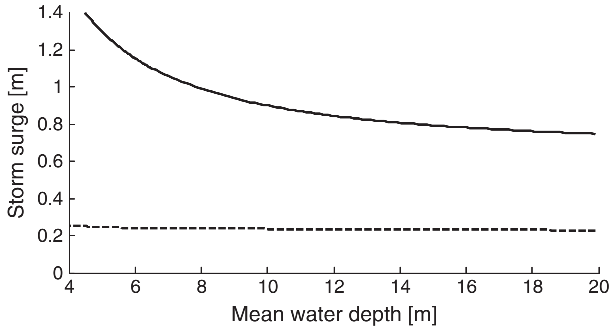

Fig. 8. Cross-shore storm surge profiles estimated for TC Roger weather conditions using air side stress $C_{10} = 2.2 \times 10^{-3}$ (— — — —) and C_{wind} (———) using the simplified continental shelf shape for the Gold Coast (Fig. 6) and Eq. (30) for air side wind stress and Eq. (31) for wave height growth inferred wind stress. The wave height and period was assumed constant across the continental shelf.

need to be added to a numerical model, with Eq. (27) concentrated at the water surface. Future development will focus in on this. For completion, 3D models will enhance the cross-shore surge component compared to 2D formulation and hence, provide a potential cancelling component of the longshore surge reductions.

The phase difference between the atmospheric pressure forcing and the wave was taken at $k\delta = \pi/2$ for maximum downwards momentum transfer. Using $k\delta \in [0.1,1]$ radians reduces the surge at 10 m water depth, when integrating over the entire continental shelf, by between 2 cm and 22 cm compared to using $k\delta = \pi/2$, yielding estimates which are still above the low-pass-filtered-storm-surge peak of 0.55 m (Fig. 9, – – – –). Consequently, these storm surge predictions are insensitive for realistic variation of $k\delta$.

Miles' normalised wind wave growth parameter β was set at 32 following Plant's (1982) recommendation of $\beta = 32 \pm 17$ and collective measurements covering $10 < \beta < 107$. Taking Plant's lower limit of $\beta = 17$ results in a 0.59 m surge at 10 m water depth. This indicates that surge predictions are sensitive to β and consequently more investigation is required.

When meteorological systems cross the coast, the character of the surge forcing changes from being a combination of cross-shore wind stresses and long-shore wind-driven currents (Coriolis force) to cross-shore wind stresses (usually the wind direction near the largest storm surges are shore normal) and reduced atmospheric pressure. Another complication is that as the forcing system approaches the coastline, the geometry (e.g., water depth contour shapes and shape of the pressure distribution) plays an ever increasing role in determining the storm surge (e.g., propagation of generated shelf waves and the longshore spatial gradients in wind stress). The final difference will be the wind-waves themselves. They will be undergoing refraction, shoaling, reflection and several types of dissipation. It is questionable if the quasi-equilibrium approach suggested applies or if the wind is still generating wave growth. Further investigation is required to resolve the question of why storm surge estimates are generally acceptable for weather systems that cross the coastline despite the use of momentum transfer based on air side wind stress.

4. Implications of the new wind stress model

The statistical modelling (Hardy et al., 2004) for Surfers Paradise, Gold Coast, Australia (Fig. 10, blue and black continuous lines), while estimated using limited engineering resources and storm scenarios, provides very different surge probabilities compared with six historical events (Fig. 10, dashed lines). The storm surge magnitudes are under-predicted significantly for a given return period. The flooding potential is also probably under-estimated, that is combining deterministic tidal variation. The five historical events shown occur over a 43 year period, with the rarest event (TC Dinah) having a bias probability of 1 in 43 in historical terms, which is well in excess of 1 in 1000 as suggested by the statistical modelling. Ruling TC Dinah out as an exceptionally rare event, while improving matters slightly, still results in TC Roger's bias probability of 1 in 36 being substantially greater than the 1 in 800 from the statistical modelling.

The air side wind stress yielded a 0.24 m surge for TC Roger, and from the statistical modelling this is approximately a 10 year event. Alternatively, using the wind stress estimated from the wind-wave growth data yields a surge between 0.9 m and 1.15 m. If we assume that the system is linear (which from Eq. (29) is a poor assumption), an increase of the statistical surge magnitudes by $(0.9 + 1.15)/2 - 0.24$~0.79 m provides a ballpark estimate of the probabilities that would be obtained when using wind stresses based on wind-wave growth observations. This ad hoc approximation is for illustration only, and is quite inconsistent with the historical events compared to TC Roger's bias return period of 36 years. It does, however, clearly indicate that TC Dinah is an exceptionally rare event (i.e., not a representative sample from the underlying distribution given the sample period).

5. Summary and further work

The storm surge resulting from tropical cyclones or East Coast Lows that travel well offshore of the eastern Australian coastline are unexplained when the momentum transfer from atmosphere to ocean uses the air side wind stress coefficient (Donelan et al., 2004). These storm surges are qualitatively explained when the factor two to three larger momentum transfers from the wave growth data (Belcher and Hunt, 1998) are used (Fig. 9). Using the wave growth measurements requires a plausible and physical link between the normalised wave growth parameter β and the input of momentum to the water column, i.e., the trough level Reynolds stress. This link was established by Nielsen et al. (2011) for the shallow water depth limit using potential flow to estimate the oscillatory motion Reynolds stresses τ_{wave}. We extend their potential flow solution to arbitrary depths and levels. This extension warrants more field measurements of Reynolds stresses across the continental shelf.

The application so far has been limited by holding the wave height and period constant across the 42 km wide continental shelf and

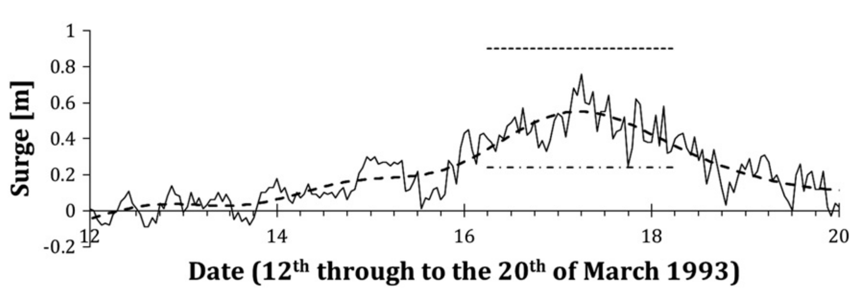

Fig. 9. Measured (non-filtered ———, and low-passed-filtered – – – –) and predicted (air side wind stress coefficient – – –, variable wave growth wind stress coefficient, both at 10 m water depth - - - - -) storm surge during TC Roger (March 1993) at the Gold Coast Seaway, Australia (Stewart et al., 2010).

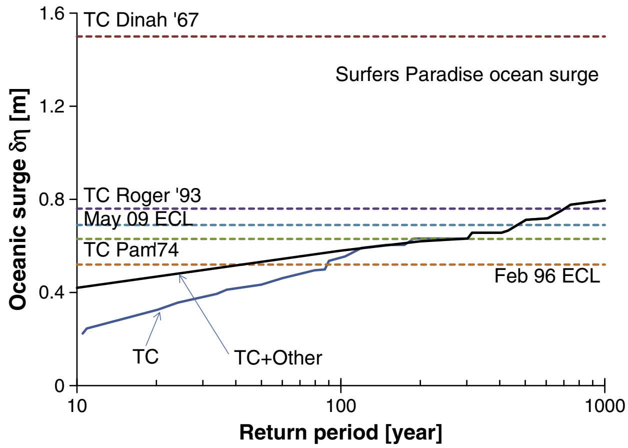

Fig. 10. Oceanic surges at Surfers Paradise from tropical cyclones Dinah, Pam and Roger and East Coast Lows (ECL) in Feb 1996 and May 2009 compared with the statistical modelling (Hardy et al., 2004). The dashed horizontal lines are the historical events, the blue continuous line is the tropical cyclone statistical predictions, the black line is an adjustment to include other meteorological events (e.g. ECL).

modelling the storm surge using two-dimensional steady shallow water equations. The storm surges are overestimated using the wave height growth data. We tested two possible reasons for this overestimate. Firstly, assuming depth averaged conditions (i.e., shear stress applied at the surface is available to drive currents over the entire depth) over the whole continental shelf. From a simplistic analysis method, we showed that surge predictions could be lowered by up to 0.3 m, bringing estimates towards the observed storm surge. Secondly, we applied the maximum momentum transfer possible. Reducing the wind-wave phase difference, and hence reducing the momentum transfer, was found to yield moderate surge reductions. Finally, surge was sensitive to Miles' normalised wind wave growth parameter β, which has substantial scatter ($10<\beta<107$). Consequently, to improve the wind stress model presented, further work (analytical, laboratory and field case studies) will be required.

Why are storm surge estimates generally acceptable for weather systems that cross the coastline despite the use of momentum transfer based on air side wind stress? We suggest the answer lies in the different forcing mechanisms generating the surge (i.e., Coriolis force phasing out and atmospheric pressure phasing in as the system crosses the coastline), the near shore bathymetry and the near-shore wind-wave behaviour. To resolve this question, additional Reynolds stress field measurements taken offshore and near the surf zone will be necessary.

While there are many outstanding issues surrounding this approach, testing provided here has, for the authors, demonstrated that there is merit in pursuing storm surge estimates forced by wind stresses obtained using the implied wind stress coefficients from wave growth observations.

References

Belcher, S.E., Hunt, J.C.R., 1998. Turbulent flow over hills and waves. Annual Review of Fluid Mechanics 30 (1), 507–538.
Carter, T.G., Liu, P.L.F., Mei, C.C., 1973. Mass transport by waves and offshore bed-forms. Journal of the Waterways, Harbours and Coastal Division 99, 165–184.
Cartwright, N., Callaghan, D.P., Nielsen, P., 2009. Coastal Field Research Facility: the Spit, Gold Coast, Australia, Civil Engineering Bulletin 25. The University of Queensland, Brisbane.
Cavaleri, L., Zecchetto, S., 1987. Reynolds stresses under wind waves. Journal of Geophysical Research 92 (C4), 3894–3904.
Donelan, M.A., Haus, B.K., Reul, N., Plant, W.J., Stiassnie, M., Graber, H.C., Brown, O.B., Saltzman, E.S., 2004. On the limiting aerodynamic roughness of the ocean in very strong winds. Geophysical Research Letters 31 (L18306), 1–5.
Hardy, T.A., Mason, L.B., Astorquia, A., 2004. Queensland Climate Change and Community Vulnerability to Tropical Cyclones: Ocean Hazards Assessment-Stage 3—the Frequency of Surge Plus Tide during Tropical Cyclones for Selected Open Coast Locations along the Queensland East Coast. Department of Natural Resources and Mines, Brisbane, Queensland.
Longuet-Higgins, M.S., Stewart, R.W., 1960. Changes in the form of short gravity waves on long waves and tidal currents. Journal of Fluid Mechanics 8 (04), 565–583.
Longuet-Higgins, M.S., Stewart, R.W., 1964. Radiation stresses in water waves; a physical discussion with applications. Deep Sea Research 11, 529–562.
Lundgren, H., 1963. Wave thrust and wave energy level. London Proceeding of the 10th International Association of Hydraulic Research, pp. 147–151.
Melville, W.K., 1996. The role of surface-wave breaking in air–sea interaction. Annual Review of Fluid Mechanics 28 (1), 279–321.
Miles, J.W., 1957. On the generation of surface waves by shear flows. Journal of Fluid Mechanics 3, 185–204.
Mitsuyasu, H., 1985. A note on the momentum transfer from wind to waves. Journal of Geophysical Research 90 (C2), 3343–3345.
Nielsen, P., 2009. Coastal and estuarine processes. Advanced Series on Ocean Engineering. World Scientific, Singapore. 341 pp.
Nielsen, P., Callaghan, D.P., Baldock, T.E., 2011. Downward transfer of momentum by wind driven waves. Coastal Engineering 58, 1118–1124.
Peirson, W.L., Garcia, A.W., 2008. On the wind-induced growth of slow water waves of finite steepness. Journal of Fluid Mechanics 608, 243–274.
Plant, W.J., 1982. A relationship between wind stress and wave slope. Journal of Geophysical Research 87 (C3), 1961–1967.
Sanchez-Arcilla, A., Collado, F., Rodriguez, A., 1992. Vertically varying velocity field in q-3d nearshore circulation. Proceeding of the 23rd International Conference on Coastal Engineering. ASCE, Venice, pp. 2811–2824.
Sheng, Y.P., Zhang, Y., Paramygin, V.A., 2010. Simulation of storm surge, wave, and coastal inundation in the northeastern Gulf of Mexico region during hurricane Ivan in 2004. Ocean Modelling 35 (4), 314–331.
Shonting, D.H., 1970. Observations of Reynolds stresses in wind waves. Pure and Applied Geophysics 81 (1), 202–210.
Stewart, J.P., 2010. February 1996 East Coast Low-Storm Surge Assessment. The University of Queensland, Brisbane. 125 pp.
Stewart, J.P., Callaghan, D.P., Nielsen, P., 2010. Tropical cyclone 'Roger' storm surge assessment, School of Civil Engineering Research Report CE162. freely available from The University of Queensland, Brisbaneespace.library.uq.edu.au/view/UQ:210173.
Tilburg, C.E., Garvine, R.W., 2004. A simple model for coastal sea level prediction. Weather and Forecasting 19 (3), 511–519.
Walton Jr., T.L., Dean, R.G., 2009. Landward limit of wind setup on beaches. Ocean Engineering 36 (9–10), 763–766.